

Measuring high-precision luminosity at the CEPC

Jiading Gong¹, Jun He², Rongyan He², Suen Hou³, Quan Ji², Renjie Ma⁴, Ming Qi⁴, Haoyu Shi², Weimin Song¹, Xingyang Sun⁴, Haijing Wang², Yilun Wang⁴, Jialiang Zhang⁴, Lei Zhang⁴

¹Jilin University, Changchun, 130012, China.

²Institute of High Energy Physics, Beijing, 100049, China.

³Academia Sinica, Taipei, 11529, China.

⁴Nanjing University, Nanjing, 210093, China.

Abstract

Purpose: Luminosity measurement at the Circular Electron-Positron Collider (CEPC) is required to achieve 10^{-4} precision when operating at the center-of-mass energy of the Z-pole. Approximately 10^{12} Z-bosons will be collected to refine measurements of Standard Model processes. The design of the luminosity calorimeter (LumiCal) takes into account the geometry of the Machine-Detector-Interface (MDI) for the detection of Bhabha events. The detector simulation with GEANT predicts measurements of scattered electrons, positrons, and radiation photons.

Methods: Bhabha events are generated with the BHLUMI program. The electrons arriving at the LumiCal fiducial coverage are counted. The electron θ angle with deviation caused by multiple scattering and detector resolution shall be measured with a precision on the lower fiducial edge better than $1 \mu\text{Rad}$, which corresponds to 10^{-4} on the Bhabha cross section. On each z-side, the LumiCal design features two silicon position detectors to measure electron impact positions, and $2 X_0$ LYSO bars behind for e/γ identification. The $13 X_0$ LYSO calorimeter mounted in front of the quadrupole magnet measures electron energy.

Results: The luminosity measurement derived from Bhabha event counting relies on the low- θ fiducial edge with a mean of better than $1 \mu\text{Rad}$. Both the beam monitoring on the interaction point (IP) and the LumiCal Si-wafer positions shall be monitored to a mean of better than $1 \mu\text{m}$. The beam-pipe design is optimized with a low-mass window of less than 2 mm thick Be window for calibration of multiple scattering. With Si-layers capable of $5 \mu\text{m}$ resolution, the error on the mean of fiducial edges is measured to $1 \mu\text{m}$. The detector displacement requires survey monitoring to sub-micron precision.

Conclusion: The scattered electrons at IP are measured with the LumiCal Si-wafers and high granularity of LYSO bars. The accompanying photon with larger opening angles can be identified and studied for radiative Bhabha events. The NLO calculations for the Bhabha interaction are achieving 10^{-4} . With the LumiCal design of silicon detectors and LYSO calorimeters, the precision is pursued for IP and detector positions being monitored, to achieve the goal of 10^{-4} precision on luminosity measurement.

Keywords: CEPC: Accelerator luminosity; Bhabha interaction

Introduction

The Circular Electron Positron Collider (CEPC) is proposed as a Higgs factory, targeting an instant luminosity of $5 \times 10^{34} / \text{cm}^{-2} \text{s}^{-1}$ at a center-of-mass energy of 240 GeV. The operation at the Z-pole with the instant luminosity of $1.15 \times 10^{36} / \text{cm}^{-2} \text{s}^{-1}$ will produce 2.5×10^{12} Z boson events [1]. With such high event statistics, the measurement of Standard Model processes will require the luminosity measurement of better than 10^{-4} precision.

The CEPC machine detector interface (MDI) region is optimized with a 20 mm diameter beam-pipe at the Interaction Point (IP), which splits into dual pipes for the 33 mRad crossing angle of electron and positron beams at ± 16.5 mRad on the x, z plane to the z -axis in the laboratory (LAB) frame. The luminometer is instrumented within the inner beam-pipe flanges at $|z| = 700$ mm and the region behind the bellow in front of the quadrupole magnets. The polar angle coverage in the LAB frame is less than 100 mRad.

The luminosity of e^+e^- colliding beams is most accurately measured using the elastic scattering events known as the Bhabha interaction. The Luminosity Calorimeter (LumiCal) is proposed for detecting back-to-back electron and positron pairs, each with momenta equal to the beam energy.

In the center-of-mass frame, the leading order Bhabha cross-section within the theta range of ($\theta_{min} < \theta < \theta_{max}$) is expressed as

$$\sigma = \frac{16\pi\alpha^2}{s} \left(\frac{1}{\theta_{min}^2} - \frac{1}{\theta_{max}^2} \right). \quad (1)$$

The integrated luminosity \mathcal{L} of e^+e^- collisions, for the number of N_{acc} Bhabha events detected is given by

$$\mathcal{L} = \frac{1}{\epsilon} \frac{N_{acc}}{\sigma}. \quad (2)$$

where ϵ is the detection efficiency. The error in luminosity is derived from Eq. 1 to be

$$\frac{\Delta\mathcal{L}}{\mathcal{L}} \sim \frac{2\Delta\theta}{\theta_{min}}. \quad (3)$$

The systematic uncertainties primarily arise from errors in the fiducial acceptance edge of θ_{min} which are caused by detector alignment offsets and position resolution when detecting electrons.

The error on luminosity is twice the error on θ at the lower edge of θ acceptance. Assuming a θ_{min} of 20 mRad, a deviation corresponding to a 10^{-4} error on luminosity is $\Delta\theta = 1 \mu\text{Rad}$. At a distance of $|z| = 1$ m from the e^+e^- interaction point, the tolerance for the survey of the detector inner edge in the transverse direction is $1 \mu\text{m}$.

In the following, we first present the “*LumiCal design*” for a luminosity calorimeter mounted on the race-track beam pipe of 10 mm inner radius. Along the x -axis, a large fraction of scattered electrons are boosted by the beam crossing and are lost in the beam pipe. For this reason, the LumiCal design has evacuated the areas adjacent to the beam pipe in $|y| < 12$ mm.

The BHLUMI event generator developed at LEP is the most effective tool for analyzing radiative Bhabha events of $e^+e^- \rightarrow e^+e^-(n\gamma)$ [2]. The precision on the Bhabha cross-section has been evaluated to be 0.037% [3]. A recently developed ReneSANCe program [4] has been reported for consistency, and provides a means for comparing the calculation of cross sections. The LumiCal acceptance for Bhabha events is evaluated with the BHLUMI, which is discussed in the “*Bhabha event acceptance*” section.

The generation of radiative photons in BHLUMI employs the Yennie-Frautschi-Suura (YFS) exponentiation algorithm [5, 6] to combine contributions of real and virtual radiation photons, with cancellation of infrared divergent terms to all orders in α . Measurement of radiative photons in Bhabha events assures the precision in theoretical cross sections and deviations in electron distributions. In the section on “*Detecting radiative Bhabha*”, photons nearby and far-off scattered electrons are identified as final state (FSR) and initial state (ISR) radiations, respectively. The distributions and measurements of radiative photons are discussed.

The detection of Bhabha events with the LumiCal is addressed in the “*LumiCal simulation*” section, which is simulated using the GEANT program [7]. The detection of electrons in Si-wafers and the electro-magnetic shower distribution in LYSO crystals are evaluated for event acceptance and systematic errors.

The upstream beam pipe material causes significant multiple scattering of electrons, resulting in a deviation of 50 to 100 mRad for a beam pipe thickness of 1 mm of Be or Al. Due to space constraints in the MDI region, the LYSO crystals are segmented into 2 X_0 bars positioned before the beam pipe flanges, and long 13 X_0 bars mounted on the front of quadrupole magnets. The front LYSO bars are segmented into $3 \times 3 \text{ mm}^2$ cells for detecting electrons and photons. Si-wafers are used to detect charged particles, helping to differentiate electrons and photons from radiative Bhabha events. The method for analyzing e/γ is detailed in the “*LYSO crystals before flanges*” section, while the measurement of the electron shower in the long LYSO bars

is discussed in the “*LYSO crystals behind Bellows*” section.

The LumiCal is designed to detect scattered electrons and photons of Bhabha events. Measuring the IP distribution depends on the beam steering and Beam Position Monitors (BPMs) for tracking beam current positions and timing of bunch crossing. Sets of BPMs are installed within the beam-pipe flanges and after the bellows surrounding individual beam pipes. The precision of measuring the θ angles of scattered electrons will rely on the distribution of IP positions, as well as the survey and monitoring of LumiCal Si-wafers. Technical details are discussed in the “*Precision on LumiCal θ acceptance*” section. The challenge for achieving 10^{-4} precision on luminosity measurement is summarized in the “*Summary*” section.

LumiCal design

The LumiCal modules in the MDI region are symmetric on both sides in z to the IP, between the Vertex-detector and the quadrupole magnets. The detector’s acceptance is favorable for lower values of θ_{min} , regarding the Bhabha cross section that has a dependence of $1/\theta^2$. The beampipe in the race-track design has an inner diameter of $\phi 20$ mm at IP, and it splits into two pipes along the x -axis toward the quadrupole magnets. A schematic representation of the MDI, in an x-z cut-view with LumiCal modules, is illustrated in Fig. 1.

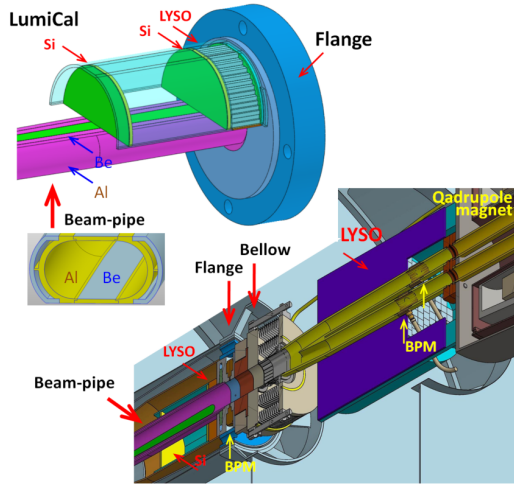


Fig. 1 The cut-view on one side of the IP is shown for the MDI region containing the LumiCal modules mounted before the flange of the race-track beam-pipe and before the quadrupole magnet. The LumiCal modules located before the flange consist of two Si-wafers and $2 X_0$ LYSO bars arranged above and below the race-track beam pipe. The green-colored Be layers serve as low-mass windows in conjunction with dual-layer Al pipes for water cooling.

On each side of the IP, the LumiCal modules are equipped with two Si-wafers and LYSO modules of $2 X_0$, positioned within the flanges above and below the race-track beam pipe. The Si-wafers are located at $|z| = 560$ and 640 mm. The flat surfaces of the beam pipe are integrated with a low-mass Be window (1 mm thick, green colored in Fig. 1) between the Al dual-layer pipes (purple colored) that contain circulating water. Behind the flanges (30 mm thick) and bellows, of a total $4.8 X_0$ steel, the long LYSO bars (150 mm in length) are mounted on the quadrupole magnets to measure scattered beam electrons.

The precision of measuring Bhabha events relies on the accuracy of detecting the positions of electron impacts at the lower θ edges of the fiducial acceptance, which are measured using the front Si-wafers. The active area is located perpendicular to the beam pipe at $|y| > 12$ mm, corresponding to $(\theta_{min} = \text{atan}(12/560))$ 21.4 mRad to the beam pipe centers. The fiducial area has a higher θ_{min} , in “ $25 < \theta < 80$ mRad” to the two beam pipe centers, and the joint rectangular area between them.

The beam-crossing of 33 mRad causes a boost to the colliding particles toward the $+x$ direction. The scattered electrons of Bhabha interactions are symmetrically distributed around the outgoing beam pipe centers on the $+x$ side. To account for the loss of electrons on the $-x$ side and ensure that electrons are detected outside the beam pipes, the fiducial edge along the x -axis is extended to $\theta_{min} = 25 + 33$ mRad. The area on the sides of the beam pipe below their height has a much smaller Bhabha cross-section, and is spared for detector implantation. The Bhabha cross-section below the height of the beam pipes ($|y| < 12$ mm) is considerably smaller, rendering those regions unnecessary for detector placement.

The detector option for detecting the impact positions of charged particles is highly advanced, utilizing Si-strip sensors that achieve precision within a few microns. This is accomplished through strips implanted at a $50 \mu\text{m}$ pitch on $300 \mu\text{m}$ thick Si-wafers. The LumiCal Si-wafers can be designed with two-dimensional strip layouts enabling the measurement of traversing particles in both the x and y directions.

The detection of electrons relies on the use of a calorimeter. The radiation-resistant LYSO crystals are chosen, which can be arranged in arrays of $3 \times 3 \text{ mm}^2$ cells with a length of 23 mm ($2 X_0$), combined with millimeter-sized silicon photomultipliers (SiPMs). These finely segmented LYSO bars are placed behind the Si-wafers, with their front surface at $|z| = 647$ mm. This setup facilitates the differentiation between electrons and photons

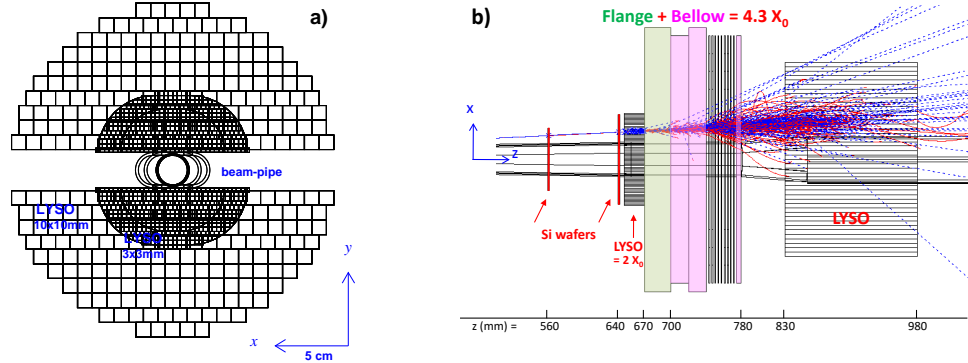


Fig. 2 The LumiCal design in the GEANT simulation is depicted in two views: a) the x - y perspective of the LYSO bars in front of the flange and behind it, with dimensions of $3 \times 3 \text{ mm}^2$ and $10 \times 10 \text{ mm}^2$, respectively, positioned above and below the race-track pipe; b) the x - z view of a 50 GeV electron shower in the Si-wafers and LYSO bars, along with the flange and bellow.

in radiative Bhabha scattering events. Scattered beam electrons shall be identified by employing elongated LYSO crystals, which capture electromagnetic shower deposits. The crystal length is restricted to 15 cm ($13 X_0$), while the dimension is configured to be $1 \times 1 \text{ cm}^2$ to approximate the Molière radius of 50 GeV electrons.

The LumiCal design has been simulated using the GEANT program [7, 8]. The layout of LYSO bars in the x - y plane is illustrated in Fig. 2.a. The event display of a 50 GeV electron shower is plotted in Fig. 2.b, in the x - z plane that shows the particle tracks in the detector modules with two Si-wafers and $2 X_0$ thick LYSO bars in front of the beam pipe flange and bellow, of a total thickness of $4.8 X_0$ steel. The long LYSO bars are positioned behind to enhance shower containment.

Bhabha event acceptance

Bhabha scattering events are generated using BHLUMI at the Z-pole energy $\sqrt{s} = 92.3 \text{ GeV}$, with default program parameters. The θ angle range specified for the Bhabha cross-section is set for 10 to 120 mRad in the center-of-mass frame. The program produces events in a wider θ range ($7 < \theta < 240 \text{ mRad}$). The final state electrons and photons are boosted for the 33 beam-crossing. Plotted in Fig. 3 are the angular distributions of scattered electrons. The θ angle of electrons is deviated by boosting by a maximum of $\pm 16.5 \text{ mRad}$. The distributions are also plotted for electrons in the fiducial region of $r > 25 \text{ mRad}$ to the beam pipe centers (red marks), and for Bhabha events selected with both back-to-back electron and positron detected in the LumiCal coverage of $|y| > 25 \text{ mm}$ at $|z| = 1 \text{ m}$ (blue marks).

The distributions of Bhabha scattering electrons in the x - y plane are plotted in Fig. 4, with the electron hits projected at $|z| = 1 \text{ m}$. The dashed line illustrates the fiducial range of $25 < \theta < 80 \text{ mRad}$ to the beam pipe centers and the joint rectangular regions between them. Boosted electrons are distributed around the $+x$ beam center (green points). The distribution in blue boxes illustrates events with both e^+ and e^- detected in the LumiCal coverage of $|y| > 25 \text{ mm}$.

The cross section for Bhabha scattering events within the LumiCal fiducial region has been estimated with the BHLUMI, applying selection criteria that require one or both back-to-back e^+ and e^- detected. Table 1 presents the cross sections at $\sqrt{s} = 92.3 \text{ GeV}$, with two θ thresholds of 20 and 25 mRad. The findings reveal that a lower angle of 20 mRad nearly doubles the cross-section. For events with both the electron and positron detected in the acceptance region, the areas on the sides below the beam pipe ($|y| < 20$ (25) mm, projected at $|z| = 1 \text{ m}$), contribute only a marginal gain of about

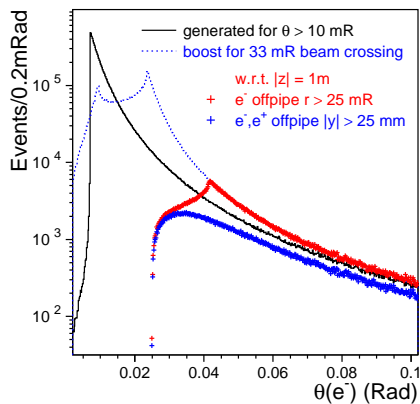


Fig. 3 Distributions in theta of scattered electrons of BHLUMI are plotted, which are generated (in 10 to 120 mRad) in the center-of-mass frame and are boosted for the beam crossing of 33 mRad. The data points in red are electrons selected outside the beam pipe with $\theta > 25 \text{ mRad}$ to the beam pipe centers (and $|y| > 25 \text{ mm}$ in between, projected at $|z| = 1 \text{ m}$). Bhabha events with both electrons and positrons detected in detector fiducial of $|y| > 25 \text{ mm}$ (projected at $|z| = 1 \text{ m}$) are plotted in blue.

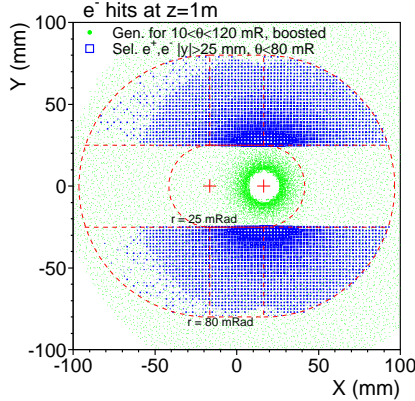


Fig. 4 The green points are electron hits generated using BHLUMI (in θ range of $10 - 120$ mRad) which are boosted and projected at $|z| = 1$ m. The blue boxes are hits with e^+ and e^- selected in the LumiCal fiducial region (in red dashed lines), for the threshold of $25 < \theta_{lab} < 80$ mRad to the beam pipe centers and the joint rectangles in between, excluding the areas below the beam pipe of $|y| > 25$ mm.

Triggered	Single e^-	both e^-, e^+
	σ (nb)	σ (nb)
$20 < \theta < 80$ mRad	217.2	140.7
and. $ y_{1m} > 20$ mm	137.5	131.2
$25 < \theta < 80$ mRad	133.4	85.9
and. $ y_{1m} > 25$ mm	82.2	78.1

Table 1 The LumiCal acceptance has been analyzed for the Bhabha scattering electrons generated with the BHLUMI in the θ range of 10 to 120 mRad. Events are selected with one or both e^- and e^+ detected in the LumiCal acceptance. The cross-sections are listed for the two θ thresholds of $20, 25 < \theta < 80$ mRad, and the joint rectangles between them (dashed lines plotted in Fig. 4). Excluding the horizontal areas below the beam pipe ($|y_{1m}| = 20, 25$ mm projected at $|z| = 1$ m), the cross-sections with both e^- and e^+ detected are about 10% lower.

10%. With the θ threshold of 25 mRad above the beam pipe, the LumiCal achieves a cross-section of 78.1 nb, requiring both e^+ and e^- detection. This value is nearly twice the $Z \rightarrow qq$ cross section (41 nb), enabling precise luminosity measurement for Z -boson line shape studies.

Detecting radiative Bhabha

Bhabha events are selected requiring the detection of both the e^+ and e^- that are scattered back-to-back in directions. One of the dominant uncertainties is the contribution of radiative production with photons in the final state. The distributions of e^+ and e^- opening angles, generated with the BHLUMI, are compared in Fig. 5. The deviations in the back-to-back angle are caused by events having radiative photons.

The BHLUMI is developed with a theoretical precision reported for 0.037% [3]. The higher-order calculation has included photonic $\mathcal{O}(\alpha^2 L)$ and hadronic $\Delta\alpha_{had}$ corrections. The cross-sections calculated at various \sqrt{s} are compared with the ReneSANCe for the θ range of 30 mRad to $\pi/2$. Illustrated in Fig. 6 are the results and the ratios of them to demonstrate the good agreement.

The BHLUMI calculation utilizing YFS exponentiation has the photon generations of $e^+e^- \rightarrow e^+e^-(n\gamma)$ following a Poisson distribution for photons in the final states. In each event, the photons are identified in the center-of-mass frame with the opening angles being closer to the incident or scattered electrons, as initial (ISR) or final state radiation (FSR), respectively.

The detection of scattered electrons and photons is analyzed applying the LumiCal Si-wafers in

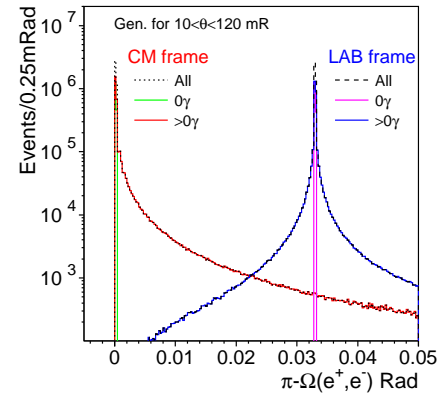


Fig. 5 The distributions of scattered e^+, e^- opening angle, generated with the BHLUMI, are plotted in the center-of-mass (CM) frame and the boosted laboratory frame. Events with radiative photons cause a deviation from the back-to-back angle of e^+ and e^- .

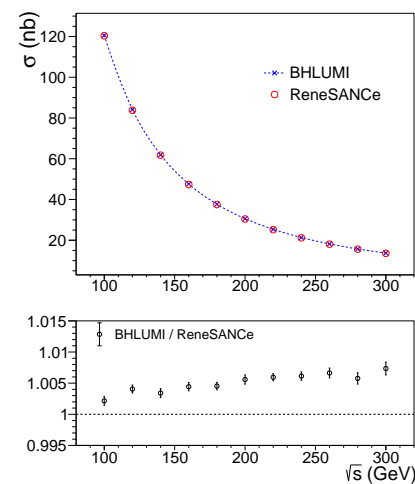


Fig. 6 Bhabha events are simulated with the BHLUMI and ReneSANCe programs, which agree well on the cross-sections plotted in a) as a function of \sqrt{s} . The ratios of them are also plotted.

front of the LYSO bars of $2 X_0$ positioned before the beam pipe flanges. The Si-wafer located at $|z| = 640$ mm has the sensitive area of $|y| > 12$ mm and an effective radius of 80 mm centered on the beam pipes, and the rectangles in between.

The Si-wafers detect electrons with ionizing charge signals while sparing neutral photons. Electrons and photons that enter the LYSO bars, segmented in $3 \times 3 \text{ mm}^2$ in the x - y plane, produce scintillation lights resulting from electromagnetic shower particles. The 3 mm pitch of the LYSO bars has a spatial resolution of 5 mRad for separating two nearby shower centers.

The BHLUMI simulations were performed at Z-pole with θ range of 10 to 120 mRad. Photons were generated with an energy threshold of 5 MeV. Scattered electrons accompanied by a photon or more in the same z -hemisphere account for 40% of the cases, with the most energetic photon being

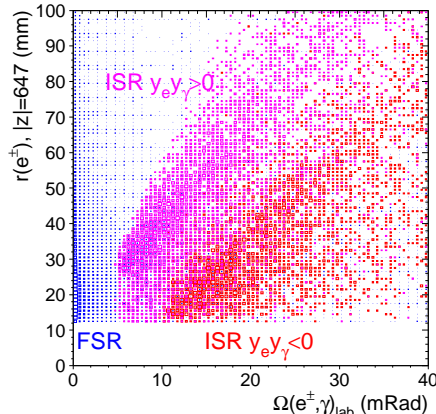


Fig. 7 Event with radiative photon ($E_\gamma > 0.1$ GeV) are selected for e^\pm and γ detected in the Si-wafer and LYSO acceptance of $|y| > 12$ mm, at $|z| = 647$ mm. The e^\pm with γ in the same z -hemisphere are plotted for the e^\pm radius to z -axis versus the e^\pm, γ opening angle. The photons are identified for FSR (blue), or ISR with the e^\pm separated on the same (red) or opposite (magenta) y -sides.

$ y(e^+) , y(e^-) , y(\gamma) > 12 \text{ mm}; E_\gamma > 0.1 \text{ GeV}$			
$e^\pm, n\gamma$	e^\pm, ISR	e^\pm, FSR	$\Omega(e, \text{FSR}) > 5 \text{ mRad}$
14.8%	0.91%	13.9%	3.0%

Table 2 Bhabha events of BHLUMI simulations in the θ range of 10 to 120 mRad are boosted for beam crossing. The inclusive Bhabha selection requires e^+ and e^- in the LYSO acceptance of $|y| > 12$ mm at $|z| = 647$ mm. In each z -hemisphere, the event fractions with a radiative photon observed in the Si-wafer acceptance are listed. The photons, being identified as an ISR or FSR, are required for $E(\gamma) > 0.1$ GeV. The event fraction containing an FSR with e^\pm, γ opening angle larger than 5 mRad is also listed. The statistical error is 0.1% on the inclusive Bhabha events.

identified as an ISR (20%) or an FSR (19%). Fig. 7 illustrates the boosted positions of e^\pm (radius to z -axis) on the Si-wafer versus the opening angle with the most energetic photon of $E(\gamma) > 0.1$ GeV in the same z -hemispheres. Events are selected with all e^+, e^-, γ falling in the LYSO acceptance of $|y| > 12$ mm at $z = 647$ mm.

Electrons accompanied by FSR photons are detected mostly as inclusive electrons. In Fig. 7, the distribution for electrons with FSR (blue) shows a peak near the beam pipe with an opening angle approaching zero. The ISR photons are distributed at a small radius near the beam pipe, to the incident electron. In Fig. 7, electrons with ISR photons are distributed in two bands, where e^\pm and γ either align on the same y -sides or the opposite.

Table 2 lists the event fractions associated with the inclusive Bhabha selection for e^+ and e^- in the LYSO acceptance range of $|y| > 12$ mm. Photons are required for $E_\gamma > 0.1$ GeV and are detected in $|y| > 12$ mm. The event fraction with an ISR, having a large opening angle to the electron in the same z -hemisphere, is 0.91 %. Most of the FSR photons fall within the opening angle of 5 mRad (91 %). Electrons associated with an FSR that can be separated by the LYSO pitch of 5 mRad is accounted for 3.0 %.

LumiCal simulation

The Si-wafers in LumiCal are utilized to detect the impact positions of electrons. With Si-strip detectors featuring a 50 μm pitch, the expected spatial resolution for charged particles is $\sim 5 \mu\text{m}$. Due to the low incident angle of scattered electrons traversing through the beam pipe, significant deviations arise from multiple scattering effects. At an incident angle of 25 mRad, the path length within a 1 mm thick beam pipe reaches 40 mm, corresponding to a radiation length of $0.11 X_0$ for a beryllium (Be) pipe, which increases to $0.45 X_0$ for an aluminum (Al) pipe.

To reduce multiple scattering effects for electrons passing through the beam pipe, the design integrates low-mass windows of 1 mm thick Be flat panels between the semicircular double-layer Al pipe ($|x| < 6$ mm at $z = 560$ mm, Fig 1). The Al pipes are simulated as 1 mm thick layers.

The effect of multiple scattering appears as a Gaussian smearing on the particle trajectory. The impact position measured by the Si-wafers at $|z| = 560$ mm is simulated with the GEANT, applying the electrons of BHLUMI generated at the Z-pole of $\sqrt{s} = 92.3$ GeV. The deviations in θ after traversing the 1 mm thick Be or Al beam

pipe layers were analyzed. The widths of Gaussian fits to the deviations in θ are

$$52 \pm 0.6 \mu\text{Rad} \quad |x| < 6 \text{ mm (1 mm Be)}, \\ 90 \pm 0.6 \mu\text{Rad} \quad |x| > 6 \text{ mm (1 mm Al)}.$$

On the Si-wafers, the detected Bhabha electrons are populated mostly at the $|y| = 12 \text{ mm}$ edge. The errors of $0.6 \mu\text{Rad}$ are statistical, corresponding to 12k (29k) events collected in the regions of $|x| < 6 \text{ mm}$ ($|x| > 6 \text{ mm}$), respectively.

The CEPIC beam size parameters at IP are $(\sigma_x, \sigma_y, \sigma_z) = (6 \mu\text{m}, 35 \text{ nm}, 9 \text{ mm})$ [1]. The beam-crossing angle of 33 mRad results in an overlap of beam bunches with the IP distribution of $\sigma_z = 380 \mu\text{m}$. For the LumiCal simulation to account for the beam size, the IP positions of Bhabha events are randomized for the beam size. The deviation of the electron trajectory increases by 5% in addition to the multiple scattering effects.

Bhabha event selection requires back-to-back e^+ and e^- pairs detected within the θ_{min} edges. The spread of electrons across fiducial edges is analyzed using BHLUMI-generated events. A Gaussian convolution with a width of $100 \mu\text{Rad}$ is applied to the θ and ϕ angles of scattered electrons to simulate multiple scattering effects. Electrons are boosted for the 33 mRad beam-crossing angle, and LumiCal acceptance is projected at $|z| = 1 \text{ m}$ with a fiducial acceptance of $|y| > 25 \text{ mm}$.

The distributions of electron impact positions on the fiducial edges are plotted in Fig. 8.a. For e^- selected in the region $|y| > 25 \text{ mm}$ (black dashed line), the Gaussian convolution indicates a symmetrically distributed spread with a width of $200 \mu\text{m}$ (blue line). The e^+ distribution exhibits a noticeable tail (red dotted) below $|y| = 25 \text{ mm}$ due to radiative Bhabha events. With both e^- and e^+ selected for $|y| > 25 \text{ mm}$ without applying the Gaussian convolution, the e^+ tail is suppressed (magenta) and agrees with the e^- distribution.

The effects of multiple scattering are further evaluated by comparing the data before and after applying the Gaussian convolution to electron positions. The difference is plotted in Fig. 8.b with a Gaussian fit that yields a width of $78 \mu\text{m}$. The sum of e^+ and e^- positions in y is also plotted for the back-to-back angle after Gaussian convolution. The fitted width of $132 \mu\text{m}$ serves as a calibration benchmark for LumiCal survey precision

LYSO crystals before flanges

The upstream beam pipe leading to the LumiCal is a 1 mm Be low-mass window. This design aims

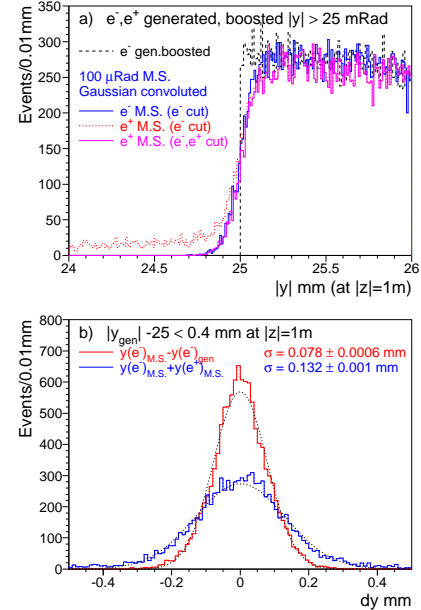


Fig. 8 The Bhabha events of BHLUMI, being boosted for the 33 mRad beam crossing, are selected for the fiducial acceptance of $|y| > 25 \text{ mm}$ at $|z| = 1 \text{ m}$. In a), the e^- selected (black dashed line) are convoluted with a Gaussian function of $100 \mu\text{Rad}$ in width on the e^\pm trajectories to simulate multiple scattering (M.S.). The resulting distributions of e^- (blue) and e^+ (red dotted) are plotted. With both e^- and e^+ selected for $|y| > 25 \text{ mm}$ before M.S. convolution, the distribution of e^+ (magenta) and e^- with M.S. convolution agree. In b), the widths of M.S. are examined. The differences in y are plotted for the e^- before and after M.S. convolution. The sum in y of e^+ and e^- is also plotted, which represents the width of the back-to-back angle affected by multiple scattering.

to minimize multiple scattering effects for traversing electrons and suppress electromagnetic showers from occurring. Electrons and photons are detected with the $2X_0$, 23 mm long LYSO arrays segmented in $3 \times 3 \text{ mm}^2$ cells, which enable e/γ separation to identify radiative photons from Bhabha scattering events.

Electromagnetic shower profiles in the LYSO array were simulated with GEANT for 50 GeV electrons at a fixed angle of $\theta = 32 \text{ mRad}$, aligned vertically to the y -axis. The shower profiles are plotted for $x-y$ and $r-z$ distributions in Fig. 9.a and b, respectively. The shower fragments are narrowly distributed within the 3 mm segmentation width. The fraction of energy deposits in the $2 X_0$ LYSO crystals constitutes approximately 1.1 % of the energy of the 50 GeV electrons.

The LumiCal is facilitated for discrimination of e/γ . The capacity was evaluated for radiative Bhabha events of BHLUMI, with the GEANT to simulate energy deposits in the $2 X_0$ LYSO crystals. Within the LumiCal acceptance of $|y| > 12 \text{ mm}$, 14% of the electrons in each z -hemisphere are accompanied by an FSR photon of $E_\gamma >$

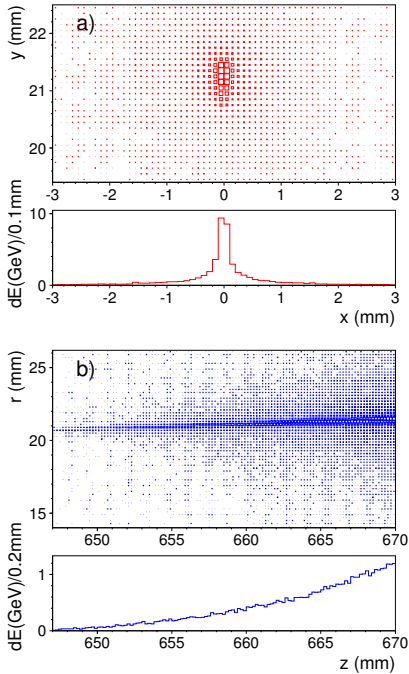


Fig. 9 Shower profiles of 50 GeV electrons in the LumiCal $2X_0$ LYSO crystal are displayed a) in the x - y plane, and b) in the r - z plane. The corresponding projected energy depositions (dE/dx) are plotted in histograms. The simulations were performed for electrons set at $\theta = 32$ mRad, vertically at $\phi = 90^\circ$ relative to the IP and traveling past a 1 mm Be beam pipe. The integrated energy deposition (dE/dx) along the z -axis through the $2X_0$ LYSO crystal accounts for 1.1 % of the electron's total energy.

0.1 GeV (Table 2). In Fig. 10.a, the energy deposits are compared for Bhabha with and without a photon in the same z -hemisphere. The separation of FSR photons from electrons is further illustrated in Fig. 10.b, in which the ratio of energy deposits in LYSO bars positioned 9 mm away ($r > 9$ mm) from the projected electron position. A prominent peak at a ratio of 0.5 indicates events with two separate shower clusters, signifying a photon located 9 mm away from the electron.

LYSO crystals behind Bellows

Bhabha events are characterized by two scattered electrons with beam energy, back-to-back in direction. In the MDI forward regions of the CEPC, located behind the beam pipe bellows, the LYSO calorimeters of 150 mm in length ($13X_0$) are accommodated in front of the quadrupole magnets. The segmentation is optimized for $10 \times 10 \text{ mm}^2$, to be larger than the Molière radius, for shower containment within a crystal bar. The long LYSOs are distinct from the $2X_0$ LYSOs before the flanges. The flange is composed of 30 mm thick steel and the Bellows of Steel and Copper (45 mm). The combined material thickness corresponding to $4.3X_0$.

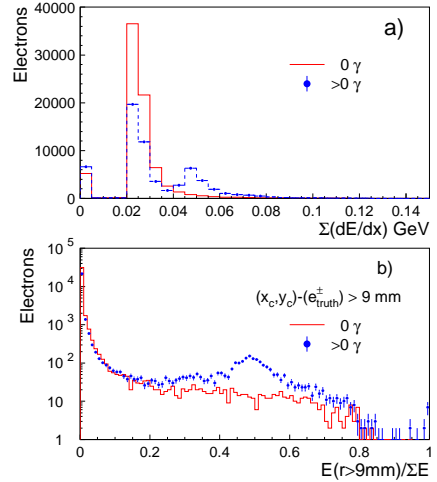


Fig. 10 Scattered electrons generated by BHLUMI, with their trajectories entering LYSO at $|z| = 647$ mm and $|y| > 12$ mm, were simulated using GEANT. The energy deposits of electrons in the $2X_0$ LYSO bars are plotted in a). The double-peak distribution for events having photons suggests observation of an electron accompanied by an FSR photon. The fraction of energy deposits in LYSO bars 9 mm off the electron trajectory is plotted in b). The bump at 0.5 indicates the observation of a photon that can be separated from the electron.

Consequently, beam electrons detected by the long LYSO calorimeters are the shower profiles after a total of $6.3X_0$.

Shower profiles in the long LYSO crystals are simulated for 50 and 120 GeV electrons. The energy deposits along the crystal length are plotted in Fig. 11.a. The electrons, injected at 44 mRad and $\phi = 90^\circ$, are fully contained in the lateral direction. The LYSO length of 150 mm contains partially the longitudinal shower profiles with the maximums ranging from 8 to $10X_0$. The energy resolution is compared for the LYSO lengths of 150 and 210 mm, which are plotted in Fig. 11.b. The Gaussian fits yield mean values of 12.5 (15.5 %) with the sample widths of 2.5 GeV (4.2 GeV) for 50 GeV (120 GeV) electrons, respectively. The energy resolution obtained with the 150 mm LYSO is 7.2 % for 50 GeV electrons, while the longer 210 mm LYSO has improved the resolution by around 1 %.

Shower containment versus the electron incident θ angle is investigated with the GEANT simulations, injecting electrons between 10 and 110 mRad at $\phi = 90^\circ$. In Fig. 11.c, the distributions are plotted for the means and standard deviations of Gaussian fits at each θ angle. A uniform plateau in shower containment is noticeable from approximately 20 mRad up to 80 mRad.

For a scattered beam electron initially at 50 GeV, a measured energy of 30.5 ± 2.2 GeV would effectively distinguish various types of background.

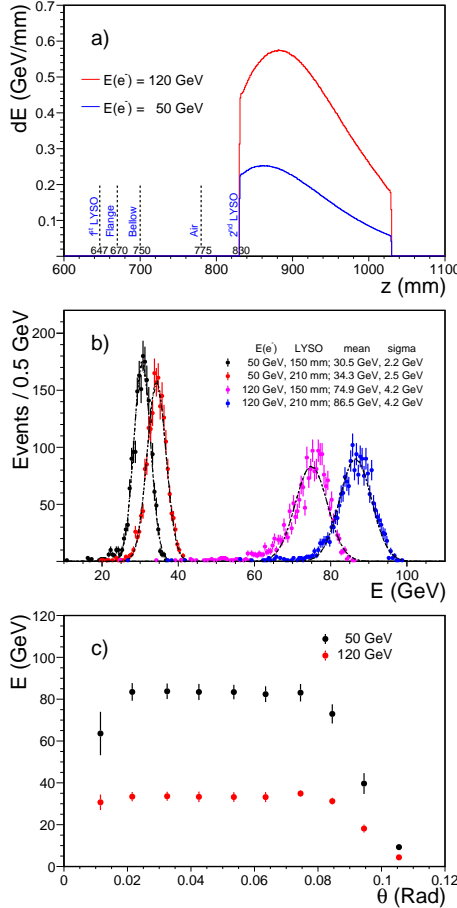


Fig. 11 The long LYSO bars positioned behind the below are simulated with lengths of 150 mm and 210 mm. The energy deposits along the z -axis are plotted in a). Energy resolutions of the sum dE/dz , fitted with a Gaussian function, are presented in b). The incident angles of the electrons are $\theta = 44$ mRad and $\phi = 90^\circ$. For LYSO bars of 150 mm in length, the Gaussian means are 30.5 (74.9) GeV, with the widths of 2.5 (4.3) GeV for 50 (120) GeV electrons, respectively. With 210 mm long LYSOs, the increase in the mean is about 15 %. Shower containment for the 210 mm LYSO is plotted in c), with the mean and standard deviations for theta values across LumiCal’s coverage. The flat plateaus of 34 (86) GeV are between the 25 and 75 mRad range.

The LYSO calorimeter with a length of 150 mm, succeeding an upstream material of $6.3 X_0$, is adequate for identifying scattered beam electrons.

Precision on LumiCal θ acceptance

The precision of luminosity measurement depends on the θ measurements of the Bhabha scattering electron and positrons within the LumiCal acceptance region, which are surveyed and monitored to sub-micron precision. The technical considerations are discussed in the following.

a. MDI LumiCal survey

The LumiCal design specifies an acceptance region of $|y| > 12$ mm on the front Si-wafers at

$|z| = 560$ mm. The overflow of scattered electrons, resulting from multiple scattering through the beam pipe, has a symmetrical distribution with a width of around 100 μ Rad. Si-detectors with a resolution of 5 μ m can measure the distribution across the fiducial edge.

The LumiCal modules, mounted on the beam pipe before the flanges, can be surveyed with sub-micron precision. Monitoring of the detector position becomes essential for calibration of the LumiCal’s fiducial edges. To achieve a precision of 10^{-4} on integrated luminosity, the errors on the means of fiducial edges are required for less than 0.6 μ m in x and y directions, and equivalently 25 μ m in z direction (Eq. 3).

b. Beam Position Monitoring

The measurement of scattered electron direction depends on the distribution of interaction points (IPs), which is ideally centered at the beam-pipe center, as the origin of the laboratory frame. Beam Position Monitors (BPMs) are employed to measure beam current positions. Within the MDI region, the BPMs are implemented inside the flanges and positioned around single-beam pipes before the quadrupole magnets, (shown in Fig. 1).

During operation, the beam positions and angles can drift over time. The beam steering in real-time employs closed-loop feedback to maintain optimal collision parameters. The BPMs located in the flanges measure coupling signals generated by the passing of electron and positron bunches, which are used to locate the longitudinal positions of the beams. The BPMs around each beam pipe are used to measure the transverse position of the beams.

b.1 Beam Longitudinal Position

To ensure that electron and positron bunches arrive simultaneously at the IP, their longitudinal positions must be measured and adjusted in real-time by modifying the radio frequency (RF) phase in the electron and positron rings, which alter their arrival time at the IP, as depicted in Fig. 12.a. The BPMs in the flanges at $|z| = 685$ mm measure the relative timing between the electron and positron bunches to determine their longitudinal positions. Assuming that the colliding bunches pass the BPMs in the flanges at t_{e^-} and t_{e^+} on each side. To arrive at the IP simultaneously, the time intervals between the crossing bunches shall be exactly $\Delta t = t_{e^+} - t_{e^-} = 2 \times 685 \text{ mm} / (3 \times 10^8 \text{ m/s}) = 4.566 \text{ ns}$.

The IP offset in z is required for $\Delta z < 25 \mu\text{m}$, which corresponds to the 1 μRad on the LumiCal acceptance edge. The error on the mean of Δt shall be better than 0.8 ps.

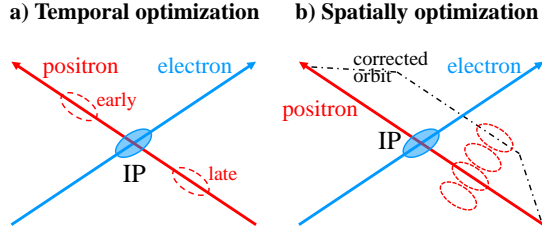


Fig. 12 Beam steering and measurements with BPMs are illustrated. a) Temporal optimization is conducted with the BPMs in flanges on the timing of the crossing bunches at IP. b) The transverse positions of the electron and positron beams in each beam are measured by the BPMs on each side of the IP, with the orbit being deviated (dashed line) by corrector magnets to be centered within the beam-pipe.

b.2 Beam Transverse Position

Ideally, the IP position should be centered within the beam pipe at coordinates $(x, y) = (0, 0)$, which assures $\Delta z = 0$. A beam-beam scan (BBS) technique is utilized to monitor and measure deviations in the transverse beam position at the IP. The beam orbits are tuned with corrector magnets near the IP, and the sets of four BPMs positioned around each beam pipe at $|z| = 1000$ mm are used to measure the beam transverse position.

In Fig. 12.b, a "bump" (represented by a dashed line) demonstrates how corrector magnets adjust the orbit in one ring. By scanning the amplitude of this bump, the transverse position can be optimized [9].

Summary

The instrumentation of LumiCal in the CEPC MDI region is being evaluated for its ability to detect small-angle Bhabha scattering events, which serve as a reference for measuring beam interaction luminosity. Achieving a precision of better than 10^{-4} for integrated luminosity at the Z-pole is critical for enhancing the accuracy of Standard Model measurements by an order of magnitude or more.

The QED calculation of the Bhabha cross-section, as implemented in the BHLUMI generator, has achieved a precision of 0.037 %. In this context, the design of LumiCal is optimized for e/γ separation, enabling accurate measurement of radiative Bhabha events.

To reach a luminosity precision of 10^{-4} , the lower θ acceptance edge at 20 mRad must be controlled with a precision of 1 μ Rad. Systematic effects related to the beam-pipe induced multiple scattering are analyzed. The position of LumiCal requires surveying and monitoring with an error on the mean of less than 1 μ m. Additionally, measurement of the IP is crucial, with beam steering and

monitoring by BPMs to an accuracy of better than 1 μ m. Meeting these stringent precision requirements demands meticulous integration of LumiCal with the beam pipe and beam steering systems to achieve sub-micron accuracy.

Acknowledgments

The authors would like to thank the assistance of the CEPC accelerator group of the Institute of High Energy Physics. This work has been partially supported by the Institute of Physics, Academia Sinica.

Declarations

Conflict of interest On behalf of all authors, the corresponding author states that there is no conflict of interest.

References

- [1] J. Gao et al., "CEPC Technical Design Report: Accelerator", Radiat Detect Technol Methods, 8 (2024) 1.
- [2] S. Jadach et al., "Upgrade of the Monte Carlo program BHLUMI for Bhabha scattering at low angles to version 4.04", Comput. Phys. Commun. 102 (1997) 229.
- [3] P. Janot and S. Jadach, "Improved Bhabha cross section at LEP and the number of light neutrino species", Phys. Lett. B 803 (2020) 135319.
- [4] R. Sadykov and V. Yermolchyk, "Polarized NLO EW e^+e^- cross section calculations with ReneSANCe-v1.0.0", Comput. Phys. Commun., 256 (2020) 107445.
- [5] S. Jadach et al., "Monte Carlo program BHLUMI-2.01 for Bhabha scattering at low angles with Yennie-Frautschi-Suura exponentiation", Comput. Phys. Commun., 70 (1992) 305.
- [6] D.R. Yennie, S.C. Frautschi and H. Suura, "The infrared divergence phenomena and high-energy processes", Annals of Physics, 13 (1961) 379.
- [7] R. Brun et al., "GEANT Detector Description and Simulation Tool", CERN-W5013, (1994).
- [8] S. Agostinelli et al.", "Geant4—a simulation toolkit", Nucl. Instrum. Methods A 506 (2003) 250.
- [9] C. Zhang, L. Ma, Design and development of accelerator for BEPCII, (2011) Chapter 12, Collision Zone System